Swiss J Geosci (2013) 106:265–278
DOI 10.1007/s00015-013-0121-0

Specialization for amphibiosis in *Brachyodus onoideus* (Artiodactyla, Hippopotamoidea) from the Early Miocene of France

Maeva J. Orliac · Pierre-Olivier Antoine · Anne-Lise Charruault · Sophie Hervet · Frédéric Prodeo · Francis Duranthon

Received: 28 October 2012 / Accepted: 25 February 2013 / Published online: 16 November 2013

Abstract A partial cranium of a very large anthracothere was unearthed during a palaeontological excavation at Saint-Antoine-de-Ficalba (Lot-et-Garonne, France; Early Miocene, ~18–17.0 Ma). The new material, referred to as *Brachyodus onoideus* (Gervais, 1859), documents the cranial features of this species, so far mainly known by dental and postcranial remains. The preserved part of the skull roughly coincides with the neurocranium and is remarkable for the dorsally-protruding orbits, the importance of the postorbital constriction, the small volume of the braincase, and the gigantic size of the occipital condyle relative to the other elements of the neurocranium. A very careful dissection of the left auditory region allowed extraction of the left petrosal bone and provides the first description of a petrosal for *Brachyodus*. The morphology of the petrosal is strikingly similar to that of extant hippos with: (1) a ventral basicapsular groove, (2) a sharp crista petrosa, (3) a wide prefacial commissure fossa, (4) a reduced mastoid, and (5) an hyperinflated tegmen tympani. Both the disposition of the orifices of the head and the petrosal morphology support a specialization of *Brachyodus onoideus* to an amphibious lifestyle and to potential underwater directional hearing.

Keywords Anthracotheriidae · Middle ear · Burdigalian · Underwater directional hearing

1 Introduction

The renovation of the RN21 motorway between Villeneuve-sur-Lot and Agen (SW France) led to the discovery by one of us (FP) of a new rich vertebrate locality west to the Saint-Antoine-de-Ficalba village (0.712°E, 44.336°N; Fig. 1). The fossiliferous exposure is a thin stripe, ~2.6 km-long (North–South) and 60/110 m-wide (East–West). Fossil-yielding deposits consist of non-indurated mica-rich sands and siltstones of fluvio-lacustrine origin, known for decades to be late Early Miocene in age (Burdigalian). Fossil remains were found scattered all over the concerned surface; no significant accumulation, anatomical connection, or bone bed was identified during the excavation undertaken in July 2008. The vertebrate assemblage of Saint-Antoine-de-Ficalba consists primarily of an abundant chelonian fauna, widely dominated by the Early Miocene land-dwelling tortoise *Testudo promarginata* von Reinach, 1900 (complete shells), but also including an aquatic/terrestrial testudinid (*Ptychogaster* sp.; connected plates) and a strictly aquatic softshell turtle (*Trionyx* sp.; connected carapace), both of poor

Editorial Handling: D. Becker & D. Marty.

M. J. Orliac (✉) · P.-O. Antoine · A.-L. Charruault
Institut des Sciences de l'Évolution, UMR-CNRS 5554,
CC064, Université Montpellier 2, Place Eugène-Bataillon,
34095 Montpellier, France
e-mail: maeva.orliac@univ-montp2.fr

M. J. Orliac
Department of African Zoology, Royal Museum for Central
Africa, Leuvensesteenweg 13, 30080 Tervuren, Belgium

S. Hervet
Association Paléovergne, 24 avenue de l'Abattoir,
03450 Ebreuil, France

F. Prodeo
Institut National de Recherches Archéologiques Préventives,
156 avenue Jean-Jaurès, 33600 Pessac, France

F. Duranthon
Muséum d'Histoire Naturelle/AMIS-UMR 5288 CNRS,
35 Allées Jules-Guesde, 31000 Toulouse, France

biostratigraphical use (Table 1). Among mammals, the rhinocerotids *Diaceratherium aurelianense* (Nouel, 1866) and *Protaceratherium minutum* (Cuvier, 1822), the cervid *Procervulus* sp., the moschid *Amphitragulus* sp., the suid *Aureliachoerus* sp., and the stem cricetid rodent *Eucricetodon infralactorensis* (Viret, 1930) in Roman and Viret (1930) were notably recognised (Table 1). This assemblage points unquestionably to the 'base MN3-base MN4' interval, documenting the Early Orleanian European Land Mammal Age (ELMA), or the Early Burdigalian in terms of standard stages (Mein 1989; Ginsburg 1990; Bruijn et al. 1992; Antoine et al. 1997, 2000; Ginsburg and Bulot 2000; Antunes and Ginsburg 2003).

The nature of the fossil-yielding sediments (siltstones and sandstones within a clayish matrix), the co-occurrence of an alligatoroid crocodile (*Diplocynodon* sp.) with turtles of strong/strict aquatic affinities (*Ptychogaster*/*Trionyx*) and a hippo-like rhinocerotid (*Diaceratherium aurelianense*; Bentaleb et al. 2006), as well as the taphonomy of the preserved remains (chelonians: complete shells and carapaces but no connected postcranials; mammals: disconnected elements) point to a fluvial environment, with a rapid burial of the concerned specimens during a flooding episode of a wide river.

A partial cranium of a very large anthracothere, labelled MHNT SAF 001, was unearthed in Saint-Antoine-de-Ficalba during the same field season in 2008. Throughout the concerned stratigraphical interval (~18–17.0 Ma), the only anthracothere recorded in Western Europe is *Brachyodus onoideus* (Gervais 1859; Dineur 1981; Ginsburg 1990; Aguilar et al. 2003; Antunes and Ginsburg 2003; Lihoreau and Ducrocq 2007). Size and gross anatomy of MHNT SAF 001 unambiguously match those of *B. onoideus*, as illustrated by Dineur (1981). *Brachyodus onoideus* is a conspicuous element of the early Orleanian European Land Mammal Age (Ginsburg 1990; Bruijn et al. 1992). Indeed, the first appearance datum of the 'last anthracothere' of Western Europe is recorded in the locality of Brüttelen (Switzerland; von Studer 1895; Scherler 2011) dated from the base of the MN3 biozone. *B. onoideus* is very common in localities referred to the middle and upper part of the MN3 biozone (Aguilar et al. 2003; Antunes and Ginsburg 2003). Its last occurrences are in Artenay (base MN4; Loire Basin, France; Ginsburg 1990), Navère and Marsolan (Fig. 1; base MN4, Garonne Basin, France; Bulot and Ginsburg 1996; Ginsburg and Bulot 2000), Bonrepos-sur-Aussonnelle (lower MN4, Garonne Basin, France; Duranthon 1991; Antoine et al. 1997, 2000), and in the "IVb unit" of the Lisbon Miocene Series (18–17.6 Ma, Portugal; Antunes and Ginsburg 2003).

If dental remains are found all over Europe and relatively abundant, cranial remains of *Brachyodus* are very scarce in contrast (Antunes and Ginsburg 2003). Its cranial anatomy was previously described in detail by Dineur (1981), based

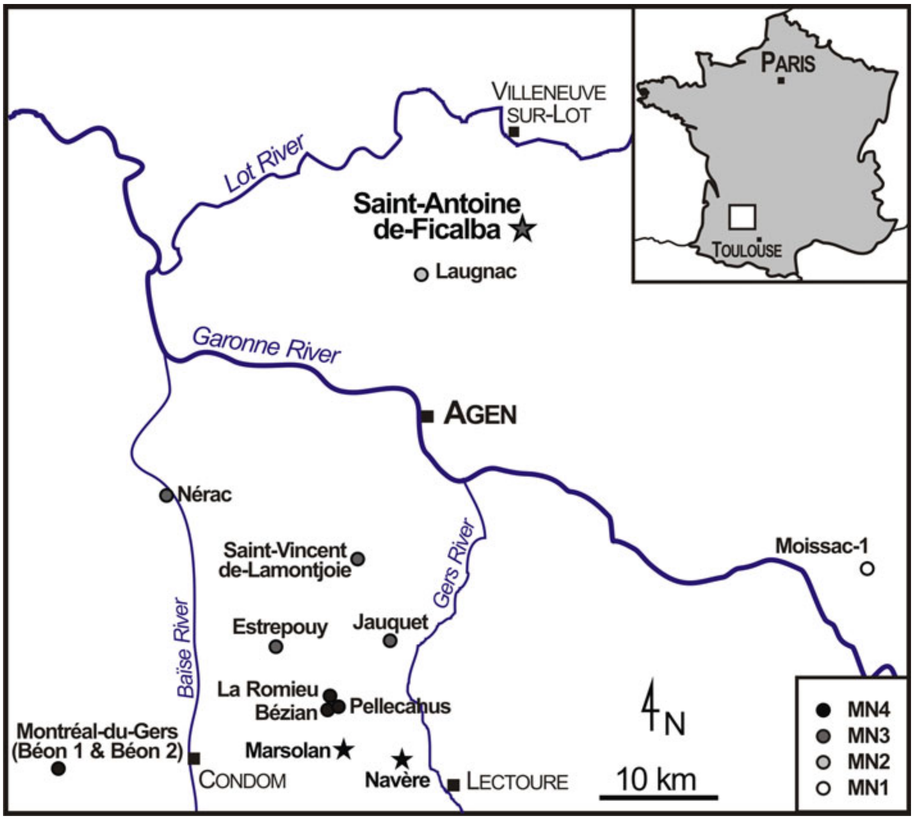

Fig. 1 Location map of Saint-Antoine-de-Ficalba (Early Miocene, upper MN3) and of selected Early Miocene vertebrate localities from the middle Garonne basin, SW France. Biochronological ages and *Brachyodus* occurrences are extracted from Baudelot and Collier (1978), Ginsburg (1990), Duranthon (1991), (Bruijn et al. 1992), Antoine et al. (1997, 2000), Ginsburg and Bulot (2000), Bulot et al. (2009)

Table 1 Vertebrate fauna of Saint-Antoine de Ficalba, SW France (late Early Miocene, Early Orleanian, base MN3-base MN4)

Supra-familial rank	Species	Mammalian Neogene zone
Chelonia	*Ptychogaster* sp.	
	Testudo sp.	
	Ergilemys sp.	
	Trionyx sp.	
Crocodylia	*Diplocynodon* sp.	
Serpentes indet.		
Mammalia, Perissodactyla	*Diaceratherium aurelianense*	(MN3-base MN4)
	Protaceratherium minutum	(MN1-base MN4)
	Plesiaceratherium sp. (medium-sized)	(?MN3-MN5)
Mammalia, Artiodactyla	*Brachyodus onoideus*	(MN3-base MN4)
	?*Hyotherium* sp.	(MN1-MN8)
	Aureliachoerus sp.	(upper MN2-MN5)
	Procervulus sp.	(MN3-lower MN5)
	Amphitragulus sp.	(MN1-lower MN4)
	Cainotherium sp.	(MN1-MN5)
Mammalia, Rodentia	*Eucricetodon infralactorensis*	(MN3)

The inferred stratigraphical interval, based on mammalian biochronology (Ginsburg 1990; Bruijn et al. 1992; Antoine et al. 1997, 2000; Antunes and Ginsburg 2003), is indicated in terms of Mammal Neogene biozones (MN; e.g., Mein 1989) for each biostratigraphically sound taxon

on two partial crania from Chilleurs-aux-Bois, Loiret, France (upper MN3; Antoine et al. 2000; Aguilar et al. 2003): S04600, a neurocranium broken just posterior to the orbit nowadays curated in the Naturhistorisches Museum in Basel, Switzerland (NMB), and a juvenile specimen without number, consisting of a neurocranium lacking the occipital (Pithiviers Museum, France; Dineur 1981: 22). From the same locality, Dineur (1981) also mentioned other cranial fragments from a private collection, documenting the glenoid and auditory areas (Faillie, FGE 13). We describe here a partial cranium of *B. onoideus* from the Early Miocene of Saint-Antoine-de-Ficalba, which completes our knowledge of the cranial and intracranial anatomy of the 'last anthracothere' of Western Europe. We further provide the first description of a petrosal for *Brachyodus* and discuss the aquatic affinities of *B. onoideus*.

2 Materials and methods

All the vertebrate remains from Saint-Antoine-de-Ficalba are permanently stored in the collection of the Muséum d'Histoire Naturelle in Toulouse, France (MHNT). A very careful dissection of the left auditory region allowed extraction of the left petrosal bone of MHNT SAF 001. Independently, this dissection allowed recognition of another isolated petrosal within the "isolated petrosal collection" from Chilleurs-aux-Bois stored in the NMB collections.

Descriptions of petrosals of "Anthracotheriidae" remain scarce in the literature. Among this paraphyletic family, the latter bones are known so far by an isolated specimen referred to as *Elomeryx armatus* from the White River Formation, South Dakota (AMNH-VP 579; O'Leary 2010) and by two in situ specimens of *Bothriogenys* sp. from the Jebel Qatrani Formation, Fayum, Egypt (DPC 20954, Early Oligocene, ~30 Ma; O'Leary et al. 2012) for which only the dorsomedial surface has been described. Comparisons of the petrosal within hippopotamoids are therefore limited to these two taxa and to the living hippos *Hippopotamus amphibius* and *Choeropsis liberiensis*.

In order to calculate the volume of the tegmen tympani relative to volume of the petrosal (excluding the mastoid region) following the protocol of O'Leary et al. (2012), we scanned the extracted left petrosal of MNHT SAF 001 (CTscan facility at the University Montpellier 2, RIO imaging—IBiZA plateform; 1,200 slices, voxel size 35 µm). We reconstructed the 3D model of the petrosal using the segmentation tools of AVIZO 6.3 (Visualization Sciences Group) and calculated the corresponding volumes by surface integration.

3 Systematic palaeontology

Artiodactyla Owen, 1848
Hippopotamoidea Gray, 1821 sensu Gentry and Hooker (1988)
"Anthracotheriidae" (paraphyletic)
Bothriodontinae Scott, 1940
Brachyodus Depéret, 1895
Brachyodus onoideus (Gervais, 1859)

Nomenclatural remark. The name Artiodactyla Owen, 1848 is used here to refer to the least inclusive crown clade containing *Camelus dromedarius* Linnaeus, 1758, *Hippopotamus amphibius* Linnaeus, 1758, *Sus scrofa* Linnaeus, 1758, *Bos taurus* Linnaeus, 1758, following the definition of O'Leary et al. (in press). Montgelard et al. (1997) proposed the new name Cetartiodactyla for the combined group of cetaceans and artiodactyls. Despite the subsequent widespread use of this term, the topological change of placing Cetacea several nodes within Artiodactyla was actually never grounds to retire the original name Artiodactyla. We follow O'Leary et al. (in press) and consider that the name Artiodactyla Owen, 1848 has priority over Cetartiodactyla Montgelard et al., 1997 according to rules of phylogenetic nomenclature.

3.1 Description and comparison

3.1.1 Cranium (Fig. 2)

The specimen is crushed dorsoventrally and the basicranium is slightly laterally shifted. The basicranium is preserved from the basis of the pterygoid processes to the foramen magnum. The ventral part of the cranium anterior to the basisphenoid is missing and cannot be described. On the dorsal surface, the cranium is broken anterior to the orbits following a breakage line that most probably corresponded laterally to the frontal/lacrymal suture.

In lateral view (Fig. 2e), despite of the dorsoventral crushing of the specimen, it is possible to affirm that the

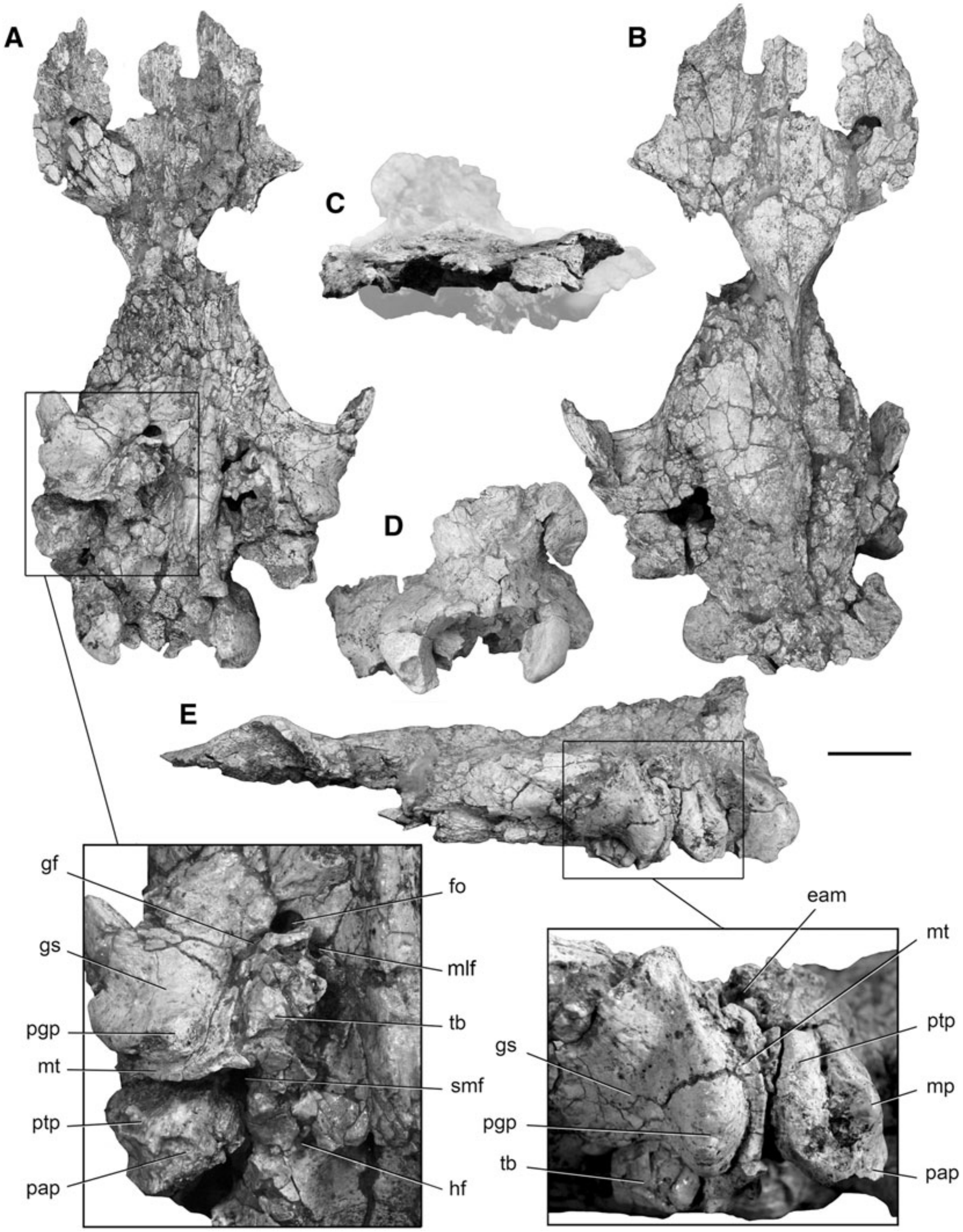

Fig. 2 Partial cranium of *Brachyodus onoideus* from Saint-Antoine-de-Filcalba (Lot-et-Garonne, France, MNHT SAF 001) in ventral (**a**), dorsal (**b**), anterior (**c**), posterior (**d**), and lateral (**e**) views. *eam* external auditory meatus, *fo* foramen ovale, *gf* glaser fissure, *gs* glenoid surface, *hf* hypoglos foramen, *mlf* medium lacerate foramen, *mp* mastoid process, *mt* meatal tube, *pap* paroccipital process, *pgp* postglenoid process, *ptp* postympanic process, *smf* stylomastoid foramen, *tb* tympanic bulla. *Scale bar* 5 cm

cranium was very low, in the same way as the undeformed specimen from Chilleurs-aux-Bois figured by Dineur (1981, pl. 8: S04600). The lateral wall of the braincase is mainly formed by the squamosal and parietal bones. However, the bad preservation of the specimen and the numerous fractures due to post-depositional processes prevent us from locating the sutures with certainty. The orbits are located in a high position and their dorsal margins protrude above the plane of the frontal (also visible in anterior view, Fig. 2c), as in extant *Hippopotamus*. On the left side of the cranium, the anatomic unit composed of the glenoid surface, meatal tube, paroccipital process, and occipital condyle is free from deformation. The postglenoid process is massive and extends ventrally to the articular surface. Posteriorly, the meatal tube is tightly imbricated between the postglenoid and postympanic processes. The external auditory meatus opens just below the temporal crest, in quite a high position, corresponding to the mid-height of the orbit. Considering this, the external ear opening of the living animal must have also opened in a high position, i.e. comparable to what is observed today in living hippos. The paroccipital process is oriented ventrally and slightly posteriorly, and is overhung by a blunt lateral tuberosity. The height between the glenoid surface and the temporal crest is similar to the total height of the large occipital condyle. The glenoid surface is located at half height of the occipital condyles. The latter are located far posterior to the occiput perpendicular.

In dorsal view (Fig. 2b), the skull is slender and elongated. The postorbital constriction is strong and the braincase maximal width is less than the frontal width anterior to the postorbital process. A strong sagittal crest runs backward from the postorbital constriction to the nuchal crest. The latter is a thin crest of bone, subhorizontal and perpendicular to the sagittal crest medially, laterally slanting ventrally and slightly anteriorly. The posterior-most part of the zygomatic arches are preserved on both sides of the cranium, broken at the level of the jugal/squamosal suture. They are only slightly diverging from the braincase, indicating that the arches were most probably not very salient laterally.

The ventral surface (Fig. 2a) of the cranium anterior to the glenoid fossa is not preserved. The basisphenoid is elongated and very narrow anteriorly; it widens posteriorly to contact the basioccipital. The latter is of constant width and bears two strong muscle insertions (for the *Musculus rectus capitis ventralis* and the *Musculus longus capitis*). The basisphenoid-basioccipital contact cannot be located precisely due to the advanced individual age of the specimen (suture fused). The posterior-most extremities of the pterygoids are preserved and they border the foramen ovale anteriorly. The latter is partially overhung by the tympanic bulla. In spite of its proximity with the medium lacerate foramen, the foramen ovale appears to be still separate from the latter by a bony crest, partially damaged on the specimen. The Glazerian fissure is visible lateral to the foramen ovale, on the right side of the neurocranium. The glenoid surface is wide and it occupies most of the ventral surface of the squamosal. On the left side of the cranium, the posterior-most part of the zygomatic arch is preserved; this structure was very light compared to the heavily built mandibular joint. The glenoid surface extends slightly anterior to the rostral part of the bulla. It is flat in its anterior portion and strongly concave posteriorly due to the presence of a strong postglenoid process. The latter is blunt and it widens medially. While there is no clear evidence of a postglenoid foramen located medial to the glenoid surface, a small foramen is observed posterior to the postglenoid process and interpreted as being the postglenoid foramen. The bulla is large, globular, and slightly elongated anteriorly. Both bullae are badly damaged, but it is possible to observe the presence of a small anterior process on the left one. The bulla is tightly apposed to the glenoid fossa anterolaterally. The meatal tube is a thick crest of bone intercalated between the postglenoid process and the postympanic process. The posterior part of the bulla is broken away and only the medial and posterior margins of the jugular notch are preserved. Laterally, between the bulla and the postympanic process, opens a wide stylomastoid foramen. The paroccipital process is mainly oriented ventrally, tightly apposed to the postympanic process of the squamosal; the tip of the paroccipital process is broken so that their total length cannot be determined.

The occipital condyles are large and massive, separated from the paroccipital process by a wide condylar fossa. The ventral surface of the occipital condyle bears a “hook-like” anterior extension, preserved on the left side of the skull. The condylar foramen is a narrow slit located lateral to the anterior extension of the occipital condyle. Its shape was probably modified by post-mortem deformation.

In caudal view (Fig. 2d), the occiput of *B. onoideus* is low and broad. The massive occipital condyles and wide foramen magnum occupy most of the posterior surface of the skull. There is a deep exoccipital fossa on the lateral border of the occipital, extending dorsally and anteriorly to the temporal crest. The foramen magnum is wider than high; it is almost straight dorsally in outline. On the dorsal side of the foramen magnum, the nuchal tubercles are blunt and weakly developed. The articular surface is composed of two convex parts forming an angle of approximately 80° and separated by a blunt oblique crest. The dorsal part of the articular surface of the occipital condyle is widely extended anterodorsally. The posterior surface of the occipital is strongly waisted above the occipital condyles. There are two wide nuchal fossae: one on each side of the

Table 2 Measurements of the cranium of *Brachyodus onoideus* from Chilleurs-aux-Bois (S04600; Dineur 1981) and corresponding values of the specimen from Saint-Antoine-de-Ficalba (MNHT SAF 001). Dimensions in mm

Measurements	*B. onoideus* Chilleurs-aux-Bois (S04600) (Dineur 1981: 31)	*B. onoideus* Saint-Antoine-de-Ficalba (MHNT SAF 001)
Maximal length of parietal bone	161	161
Minimal width at postorbital level	64	60.9 (slightly underestimated due to deformation)
Maximal width measured at posterior border of zygomatic arch	234	230 (estimation based on the left side of the skull)
Cranial width at postorbital process	154	162 (estimation based on the left side of the skull)
Minimal width between glenoid surfaces	85	81
Maximal width of the occipital at the level of the exoccipital condyles	118	125 (estimation based on the left side of the skull)
Cranial length posterior to posterior lacerate foramen (foramen jugulare)	68	72

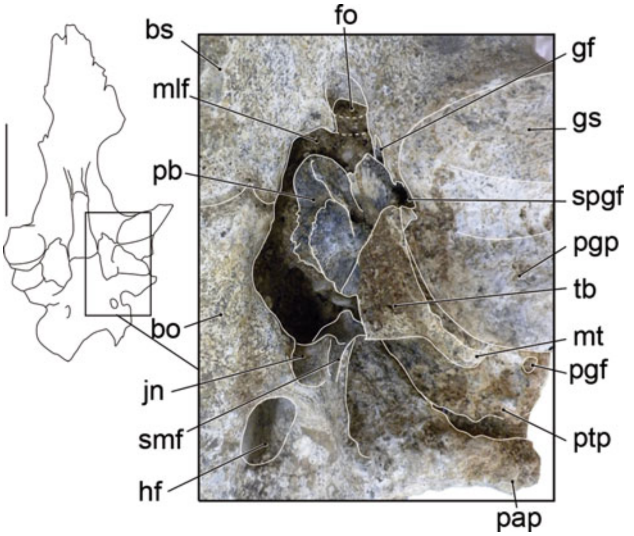

Fig. 3 Labelled detail view of the *left* auditory region of the cranium of *Brachyodus onoideus* from Chilleurs-aux-Bois (Loiret, France, NMB S04600). *bo* basioccipital, *bs* basisphenoid, *fo* foramen ovale, *gf* glaser fissure, *gs* glenoid surface, *hf* hypoglos foramen, *jn* jugular notch, *mlf* medium lacerate foramen, *mp* mastoid process, *mt* meatal tube, *pap* paroccipital process, *pb* petrosal bone, *pgf* postglenoid foramen, *pgp* postglenoid process, *ptp* postympanic process, *smf* stylomastoid foramen, *spgf* secondary postglenoid foramen, *tb* tympanic bulla. *Scale bar* 10 cm

salient nuchal tuberosity. The nuchal crest is a narrow crest of bone. The external occipital protuberance is massive, medially bordering the deep nuchal fossae.

3.1.2 *Comparisons with other cranial material of Brachyodus*

The skull from Saint-Antoine-de-Ficalba perfectly matches that of Chilleurs-aux-Bois (S04600), both for metrics and morphology, which allows us to assign the cranium from Saint-Antoine-de-Ficalba to *Brachyodus onoideus* without any doubt (for metrics comparison, see Table 2). S04600 is in a much better state of preservation than MHNT SAF 001. Accordingly, it brings some additional information to the morphological description provided here. As already mentioned by Dineur (1981), the dorsal part of the squamosal is perforated by several small foramina. Based on the juvenile specimen curated in Pithiviers, Dineur (1981) mentioned that these foramina communicate with the meatal duct, just as the postglenoid foramen. It is worth noting that Dineur (1981) mentions a foramen located medial to the glenoid surface, also communicating with the meatal duct. This foramen is illustrated in Fig. 3 with the other features of the auditory region of the skull from Chilleurs. This foramen, interpreted here as a secondary postglenoid foramen, corresponds to the medial postglenoid foramen of Geisler et al. (2007). This character is of phylogenetic importance and has been proposed as a synapomorphy shared by “anthracotheres” and cetaceans. As mentioned in the description, the specimen from Saint-Antoine-de-Ficalba does not show any clear foramen medial to the glenoid fossa, suggesting that the presence of this character might be variable, or might depend on the individual age of the specimen. S04600 also preserves both petrosals in situ, the ventral surface of which is visible in the space let by the broken bulla. This brings additional information about the in situ location of the petrosal in the cranium.

According to Lihoreau and Ducrocq (2007), only one species of *Brachyodus* is known from the Early Miocene of Europe: *B. onoideus* (Gervais, 1859). In addition, *B. aequatorialis* McInnes, 1951 occurs in the Early Miocene of east Africa, while *B. depereti* (Fourtau, 1918) and *B. mogharensis* Pickford, 1991 are identified in the late Early Miocene of Egypt. Among the non-European species, only *B. aequatorialis* is documented by good cranial remains. The holotype of the species consists in a nearly complete cranium, from the Early Miocene locality of

Rusinga (Kenya; McInnes 1951). This specimen, figured by McInnes (1951, pl. 1 and 2) in dorsal, lateral and ventral views, has undergone very little distortion. As such, it gives access to the proportions and relative position of the different elements of the cranium. The cranial features of this species are by all aspects identical to the preserved part of the cranium of *B. onoideus*. Interestingly, the anterior portion of the snout (comprising the anteriormost part of the nasals) is preserved in the specimen of *B. aequatorialis*, contrary to what occurs in MHNT SAF 001. The nasals only project over the nasal aperture on a little distance and do not reach the anterior border of the premaxillae. A premaxilla of *B. onoideus* from Chilleurs-aux-Bois figured by Dineur (1981: pl. 3) shows that the nasal opening conversely extended far back posteriorly in the latter species.

The cranial morphology of *B. onoideus* can be compared to that of *Elomeryx crispus*, an 'advanced bothriodontine' ranging from the Late Eocene up to the early Late Oligocene in Western and Southeastern Europe (MP18-26; Lihoreau and Ducrocq 2007; Lihoreau et al. 2009). An almost complete cranium of *E. crispus* was recently described from the early Late Oligocene deposits of Moissac-III, SW France (Fig. 1; Lihoreau et al. 2009).

E. crispus differs from *B. onoideus* in terms of cranial morphology in having (1) orbits much larger compared to the relative size of other elements of the cranium, (2) a higher profile of the cranium with the auditory meatus located at the level of/or slightly above the ventral and margin of the orbit, (3) a weaker postorbital constriction, and (4) a close distance between orbit and glenoid surface.

3.2 Petrosal bone (Figs. 4, 5)

The exact initial position of the petrosal in the MHNT SAF 001 cranium could not be precisely determined due to post-mortem deformation. The left petrosal protruded dorsally through the parietal bone so that parts of the parietal and squamosal bones were removed to extract the left petrosal from the endocranium. Due to the drastic reduction of the mastoid part of the petrosal, the latter did not intercalate between the squamosal and the occipital bones. Only a small spike of the tegmen tympani (broken during the dissection of the specimen) was intercalated between the meatal tube and the basis of the postglenoid process of the squamosal. Complementary information about the exact position of the petrosal in the cranium is provided by the

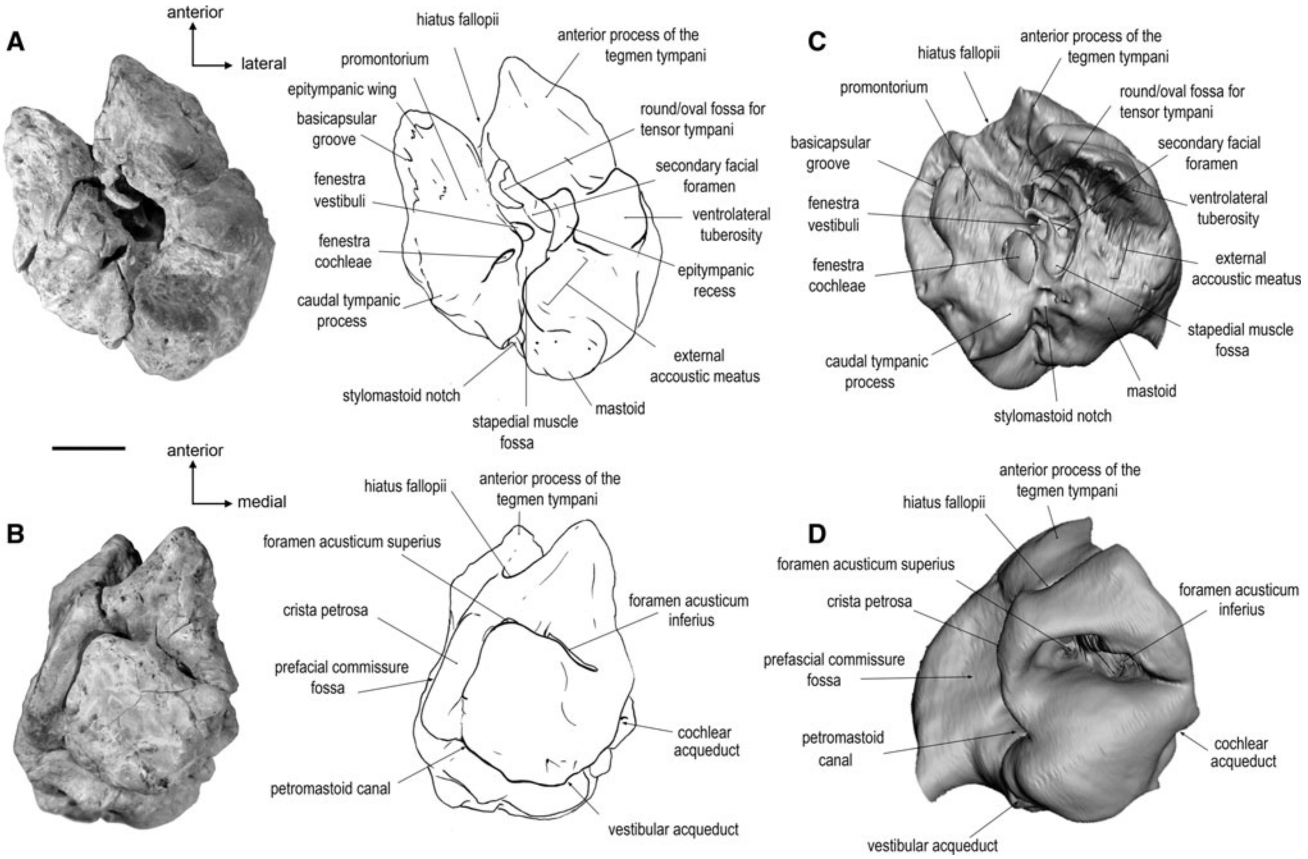

Fig. 4 Petrosal bone dissected from the cranium of *Brachyodus onoideus* from Saint-Antoine-de-Filcalba (MNHT SAF 001) in ventrolateral (**a**), and dorsomedial (**b**) views compared to the petrosal bone of the extant pygmy hippo *Choeropsis liberiensis* (M09-5-005A, Faculté des sciences, Poitiers) in ventrolateral (**c**), and dorsomedial (**d**) views. *Scale bar* 1 cm

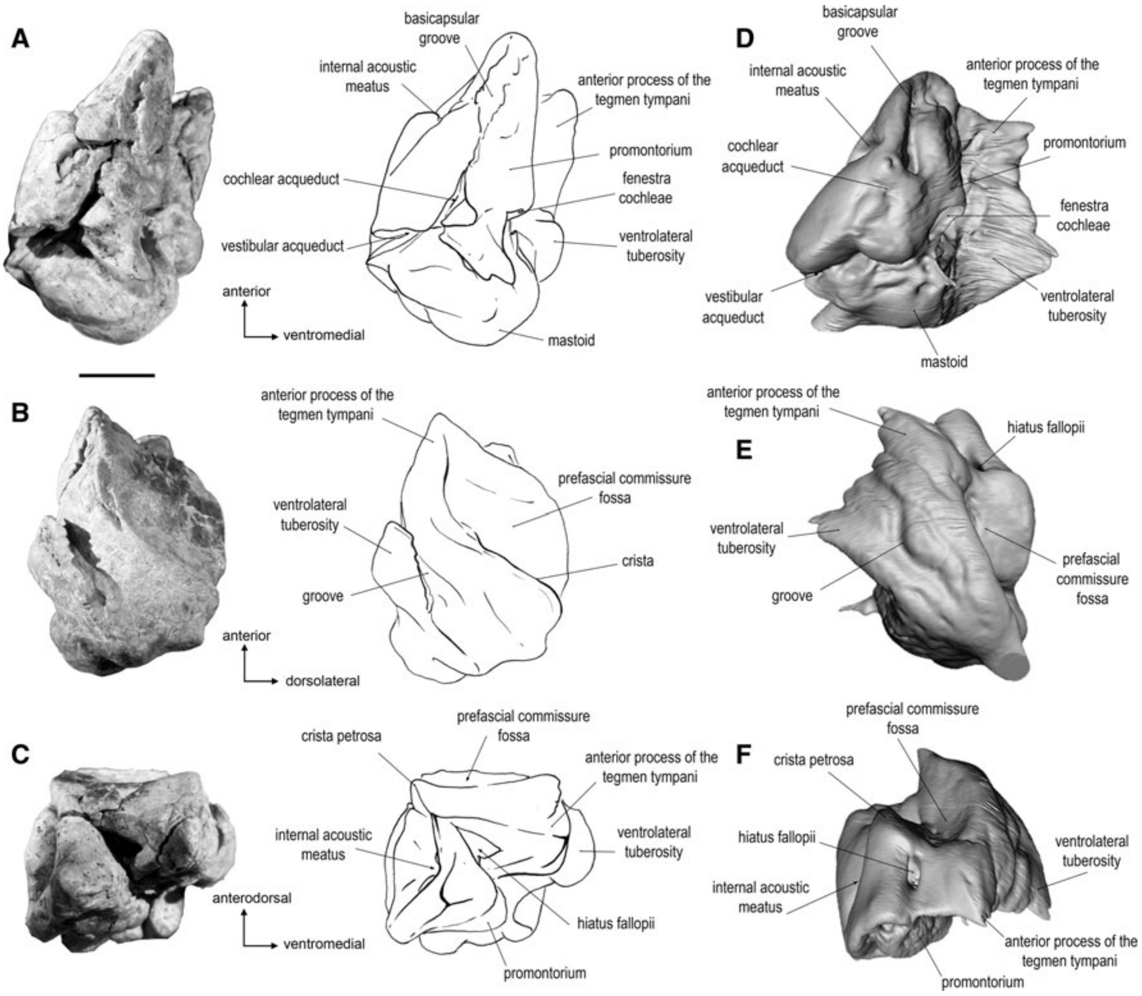

Fig. 5 Petrosal bone dissected from the cranium of *Brachyodus onoideus* from Saint-Antoine-de-Filcalba (MNHT SAF 001) in posterior (**a**), anterodorsal (**b**), and anteroventral (**c**) views compared to the petrosal bone of the extant pygmy hippo *Choeropsis liberiensis* (M09-5-005A, Faculté des sciences, Poitiers) in posterior (**d**), anterodorsal (**e**), and anteroventral (**f**) views. *Scale bar* 1 cm

ventral view of the cranium from Chilleurs-aux-Bois (Fig. 2), showing the ventromedial part of the right and left petrosals. The petrosal of *B. onoideus* is further documented by an isolated specimen from Chilleurs-aux-Bois (NMB SO 355), only lacking the anterior part of the pars cochlearis and part of the mastoid.

In ventrolateral view (Fig. 4a), the petrosal of *B. onoideus* is blunt posteriorly and shows two anterior points of equal size. The medial point corresponds to the anterior extremity of the pars cochlearis and the lateral one is formed by the gigantic tegmen tympani. The promontorium is hemi-ellipsoidal, softly inflated and medially slanting. It only extends anteriorly to half of the pars cochlearis. The anterior development of the epitympanic wing is difficult to determine: when present, it is completely fused to the anterior end of the dorsomedial surface of the petrosal. The fenestra cochleae is a small ellipsoid aperture directed posteriorly. The fenestra vestibuli is slightly larger, located beneath the fenestra cochleae, just like in living hippos (*Hippopotamus* and *Choeropsis*; O'Leary 2010, Figure 42, 48). The two fenestrae are separated by a wide crista interfenestralis. The promontorium is completely smooth and no sulci are visible. The fossa for the tensor tympani is shallow and teardrop-shaped, located lateral to the fenestra vestibuli and only expanding slightly anterior to it; its floor is broken and the secondary facial foramen canal is exposed. The fossa for the tensor tympani excavates the adjacent inflated tegmen tympani. The secondary facial foramen opens lateral to the fenestra vestibule; its anterior margin is broken, which corresponds to the anterior position according to O'Leary (2010). The promontorium gives rise anterolaterally to a long epitympanic wing merging to the dorsomedial surface of the pars cochlearis anteriorly and to a thin posteromedial flange medially, the external margin of which is broken. The latter contacts a small caudal tympanic process posteriorly. A distinct basicapsular groove runs anteroposteriorly along most of the promontorium, until the level of the caudal tympanic process (Fig. 4a). This ventral position of the basicapsular groove is also observed in living hippopotamids (Fig. 4c). The pars canalicularis is composed (1) of a reduced knob-like mastoid, cut by a wide external auditory meatus, and (2) of a gigantic and hyperinflated tegmen tympani, as wide as the pars cochlearis, extending anteriorly to the anterior edge of the petrosal. Its anterior process is a blunt spike overhanging a wide hiatus fallopii, located rather ventrally. The tegmen tympani is composed of two perpendicular/orthogonal flat areas, the dorsal one of which is slightly concave mediolaterally and also form a 90° angle with the dorsomedial surface of the pars cochlearis. The lateral part of the tegmen tympani shows a deep groove, almost closed in a canal by a bony fold just anterior to the ventrolateral tuberosity. This groove could correspond to the carotid artery. Posterior to the ventrolateral tuberosity is a large and deep depression corresponding to the petrosal contribution to the external auditory meatus. Anterolateral to it is the wide notch of the epitympanic recess. The facial sulcus is short and separated from a shallow and poorly defined stapedial muscle fossa by a small bony ridge. The stapedial muscle fossa extends to the medial margin of the fenestra cochleae. The stylomastoid notch (i.e., the petrosal contribution to the stylomastoid foramen) is wide and flat, located directly posterior to the fenestra cochleae. The mastoid region is a swollen irregular knob, not extending medially to the level of the fenestra cochleae. The tympanic bulla has a strong anterior contact with the tegmen tympani and fuses to it in the part surrounding the fossa for the tensor tympani. In ventrolateral view, the petrosal of *B. onoideus* differs from that of *Elomeryx armatus* by several features. The promontorium of *E. armatus* does not show a basicapsular groove; the latter is visible on the dorsomedial surface of the bone. The location of the epitympanic wing is more lateral and the postero medial flange is more developed in *E. armatus*. In general, the pars cochlearis of *E. armatus* is dorsoventrally thinner than that of *B. onoideus*. The development of the tegmen tympani of *E. armatus* is greatly reduced compared to that of *B. onoideus* and so does the ventrolateral tuberosity. However, relative size and location of the fenestra cochleae and fenestra vestibuli are similar in both taxa. The ventrolateral view of *Bothriogenys* has not been figured by O'Leary et al. (2012).

The dorsomedial surface (Fig. 4b) of the petrosal terminates anteriorly by a spike. The internal acoustic meatus is a transverse slit instead of the large opening traditionally present in Artiodactyla. The foramina acusticum superius and inferius are wide holes of similar size, separated by a very narrow crista transversa. The lateral edge of the foramen acusticum superius is prolonged posteriorly by a fissure lining a sharp crista petrosa (crista separating the pars cochlearis in contact with the cerebellar part of the brain and the tegmen tympani in contact with the cerebral part of the brain). This fissure, directed toward the petromastoid canal, is also observed in living hippopotamids (*Hippopotamus* and *Choeropsis*; Fig. 4d; also visible in O'Leary 2010: Figures. 44, 49). The petromastoid canal lays in a shallow depression, that might be a relic of the subarcuate fossa. Lateral to the crista petrosa, on the tegmen tympani, is a wide and shallow concavity interpreted here as the prefacial commissure fossa. The later is delimitated posteriorly by a sharp crest of bone. The position of the prefacial commissure fossa of *Brachyodus* is similar to that observed in *Choeropsis*, while this structure is located more posterodorsally in *Hippopotamus*. The small slit of the petromastoid canal is medially confluent with that of the vestibular aqueduct. The latter occupies a dorsomedial position. Just posterior to it, the mastoid shows a deep foramen. In dorsomedial view, the caudal tympanic process is visible on the posteromedial border; it marks the position of the cochlear aqueduct.

The dorsomedial surface of the petrosals of *B. onoideus* and *E. armatus* differs by the presence of a shallow but wide subarcuate fossa in *E. armatus* while only a vestigial concavity is observed in *B. onoideus*. Surprisingly, there is no petromastoid canal in *E. armatus*, contrary to what occurs in *B. onoideus*. In *B. onoideus*, the pars cochlearis occupies most of the dorsomedial surface of the petrosal, especially due to the very wide and flat portion of bone extending from the internal auditory meatus to the fissure surrounding running from the petromastoid canal to the cochlear aqueduct. This part is much less developed in *E. armatus*. According to the Figure 68 of O'Leary (2013), the location of the vestibular aqueduct in the latter is more medial than in *B. onoideus*. Despite these differences, *B. onoideus* and *E. armatus* share the presence of a straight and sharp crista petrosa. In both taxa, the vestibular aqueduct lays in a deep slit joining the cochlear aqueduct. The dorsomedial surface of the petrosal of *Bothriogenys* has been figured by a drawing by O'Leary et al. (2012: Fig. 3). From this drawing, it is possible to say that the petrosals of *B. onoideus* and *Bothriogenys* share an anterior opening of the hiatus fallopii and a hyperinflated tegmen tympani. Unfortunately, the lateral and anterior extension of the tegmen tympani cannot be observed in *Bothriogenys* as it is partly hidden by the squamosal (O'Leary et al., 2012: Figure 3). The angle between the pars cochlearis and the tegmen tympani cannot be determined either. Besides, on the tegmen tympani is a depression that could correspond to the depression described here in *B. onoideus* as the prefacial commissure fossa (i.e., lateral to the internal acoustic meatus and not posterior to it). According to the location of this fossa on the in situ specimen (O'Leary et al. 2012: Figure 3), it could well be in contact with the cerebral hemisphere while the rest of the dorsomedial surface of the petrosal would rather contact the cerebellar part of the brain, as interpreted here in *B. onoideus*. This portion of the tegmen tympani with the fossa is exposed in the internal part of the cranium, while the rest of the tegmen tympani contacts the squamosal, just like in *B. onoideus*. Contrary to what is observed in *B. onoideus* and *Bothriogenys*, the petrosal of *E. armatus* has no hyperinflation of the tegmen tympani, and no fossa on this structure. Unfortunately, the fact that this specimen is isolated makes it difficult to determine its position in situ.

The anterodorsal view (Fig. 5b) offers the best view of the gigantic tegmen tympani. The latter structure represents half of the petrosal total volume. It is parted in two by a thin but sharp crest of bone, delimitating the lateral edge of the prefacial commissure fossa. This fossa is wide and shallow in the specimen extracted from MHNT SAF 001, while narrow and slightly deeper in the SO 355 specimen (Fig. 6). The fossa is much deeper in living hippos (Figs. 4d, 5e, f). However, it occupies exactly the same position in the braincase, and contacts the posteroventral part of the cerebrum, while the crista petrosa separates the cerebral surface of the petrosal (on the tegmen tympani) from the cerebellar surface (on the medial surface of the pars cochlearis). In both specimens of *B. onoideus*, there is a strong vascular groove running on the tegmen tympani from the ventromedial edge to the posterior edge of the dorsolateral surface. This groove is also observed in living hippopotamids (Fig. 4e; O'Leary 2010: Figure 45). A groove also seems present in *E. armatus* (O'Leary 2010: Figure 69). The ventrolateral tuberosity is a rounded, knoblike, ventral protrusion in *B. onoideus*. It is also present, yet slightly smaller, in *E. armatus* (O'Leary 2010: Figure 69).

The cochlear and vestibular aqueducts are visible on the posterior side (Fig. 5a) of the petrosal of *B. onoideus*. The former is a deep and large slit located at the posterior extremity of the basicapsular groove, opening at the level of the fenestra cochleae and ventrally bordered by the caudal tympanic process. The vestibular aqueduct also emerges in a deep slit, located dorsally and posteriorly to the cochlear aqueduct. The slit is prolonged by a fissure that communicates laterally with the fissure projecting backwards from the internal auditory meatus.

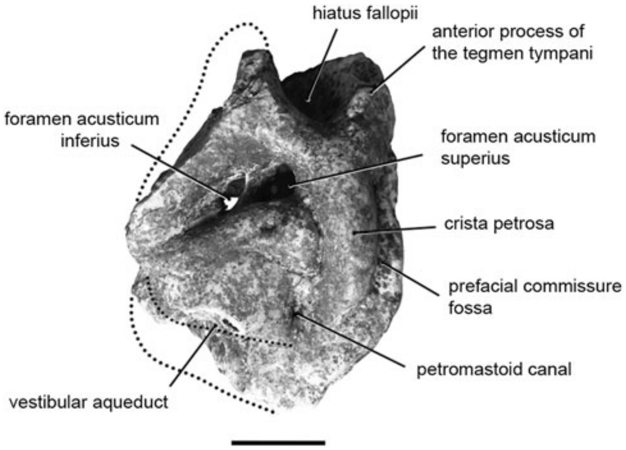

Fig. 6 Isolated petrosal of *B. onoideus* from Chilleurs-aux-Bois (NMB SO 355), in mediodorsal view. *Dotted lines* represent the external profile of the broken parts. *Scale bar* 1 cm

In anteroventral view (Fig. 5c) the hiatus fallopii is a wide triangular foramen opening slightly ventrally. The hyperinflated tegmen tympani protrudes ventrally in a large rectangular bony expansion. The thickness of the tegmen tympani oversizes that of the pars cochlearis of the petrosal. The dorsolateral surface of the tegmen tympani is in contact with the cerebral hemisphere, while the lateroventral surface contacts the squamosal. *B. onoideus* and *E. armatus* share the presence of a straight and sharp crista petrosa creating a right angle between the pars cochlearis and the tegmen tympani. This right angle is particularly visible in anterior view (Fig. 5c vs. O'Leary 2010: Figure 71).

4 Discussion

The phylogenetic affinities of the Anthracotheriidae have been subject of discussion for many years. Despite recent steps forwards (e.g., Boisserie et al. 2005, 2010; Orliac et al. 2010), the monophyly of the group is still not unanimously supported. The large scale analyses performed at the Artiodactyla level by Spaulding et al. (2009: Figure 2), combining molecular and morphological data, found anthracotheriids as a polyphyletic assemblage disseminated from the first offshoot of Ruminantia, to sister taxon to extant Hippopotamidae, or at an unresolved position at the very base of the Artiodactyla tree. On the other hand, a recent phylogenetic study based on dental evidence and including a large sample of extant and extinct Hippopotamidae (Orliac et al. 2010) supported a clade gathering the paraphyletic Anthracotheriidae and the Hippopotamidae, in agreement with Hippopotamoidea sensu Gentry and Hooker (1988). Yet, this latter analysis only included a limited sample of "non-Suiformes" taxa. Besides, the "composite phylogenetic hypothesis for Artiodactyla" of Gatesy et al. (2012: Figure 8) resulting from the combination of trees derived from three supermatrices and including both extant and extinct taxa, supports a clade composed of anthracotheriids plus *Mixtotherium* (traditionally typifying the family Mixtotheriidae; Erfurt and Métais 2007).

Interestingly, several anthracotheriids have been interpreted as amphibious animals, either based on $\delta^{18}O$ isotopic analyses (e.g., Clementz et al. 2008), or on their cranial morphology (e.g., *Libycosaurus*; Lihoreau et al.

2003). The presence of an inflated tegmen tympani of the petrosal bone, observed in both anthracotheres and living hippos, as well as in cetaceans, has also been correlated with directional underwater hearing and is another piece of evidence of specialization for an amphibious lifestyle of some "anthracotheriids" (e.g., *Bothriogenys*; O'Leary et al. 2012). Based on the results of Spaulding et al. (2009), this shared character has however been interpreted as a convergence and amphibiosis has been considered as independently acquired in anthracotheres and hippos (O'Leary et al. 2012). In the alternate hypothesis of monophyletic Hippopotamoidea (sensu Gentry and Hooker 1988), as supported by a more exhaustive sample of fossil hippopotamids and anthracotheres (Orliac et al. 2010), clarifying the life style of "anthracotheriids" is of great interest to reconstruct the evolutionary history of amphibiosis within hippopotamoids.

4.1 Semi-aquatic specialization of *Brachyodus onoideus*

4.1.1 Disposition of the elements of the cranium

The peculiar disposition of the different elements of the skull of living hippos allows them to stand in the water with their head in an "amphibious position": eyes, ears, and nostrils above water, and the rest of the body below water. In this position, they are able to breathe and see above the water surface, but also to communicate via "amphibious communication", a communication mode defined by Barklow (2004). With their ears and nostrils above water and mouth and throat below water, they produce and ear sounds in both air and underwater simultaneously (Barklow 2004). The low-frequency fast-travelling underwater sound produced by their throat travels upstream and downstream along the river and is heard by other hippos at least a mile away. This wave of "hippo calls" is interpreted as conveying information about where the individuals are at a given time, avoiding conflicts by indicating boundaries of the different territories (Barklow 2004). The peculiar morphology of the hippo skull is therefore directly related to its semi-aquatic life style.

Brachyodus has been interpreted as living in swamps or close-by rivers, but their overall more cursorial postcranial skeleton (e.g., more elongated metapodials) made them be considered as "less aquatic-adapted" than living hippos (Antunes and Ginsburg 2003). Yet, the location of the orbit of *Brachyodus*, with the dorsal edge slightly protruding above the level of the frontal, and the location of the external auditory meatus, opening at half the height of the orbit, is very close to the disposition of these elements observed in the skull of *Hippopotamus amphibius* as illustrated in Fig. 7. A premaxilla from Chilleurs-aux-Bois figured by Dineur (Dineur 1981: pl. 3) shows that the medial suture between premaxilla was high and vertical, and that the nasal opening extended far back posteriorly, which is compatible with a dorsal opening of the nostrils in this taxon. The anterior part of the snout of *B. aequatorialis* figured by McInnes (McInnes 1951: pl. 1) further indicates that the anterior extension of the nasal was concurrently very short in *Brachyodus*, another element compatible with a high location of the nostrils. Taken together, the different elements of the cranium known for *B. onoideus* (and *B. aequatorialis*) allow proposing a reconstruction of the skull as illustrated in Fig. 7b, and makes plausible the hypothesis of an alignment of nostril-eye-ear, and therefore, an "amphibious position" of the head in this taxon.

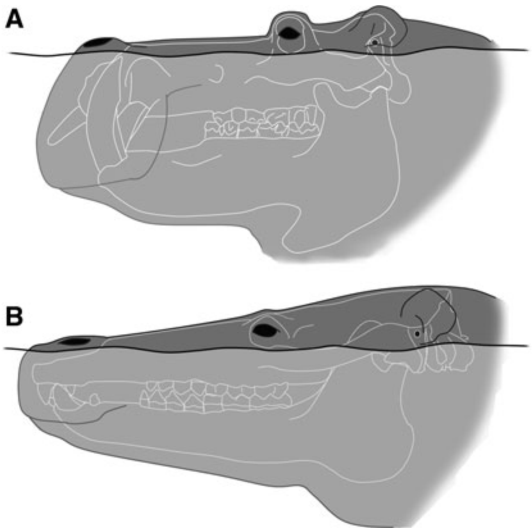

Fig. 7 Sketch of the *left* profile of the skull of *Hippopotamus amphibius* illustrated in an "amphibious position" (**a**), and reconstruction of the corresponding profile of *Brachyodus onoideus* (**b**). The *undulated line* represents the water surface

4.1.2 Middle ear morphology and ability for underwater directional hearing

The fact that *Hippopotamus* individuals can vocalize underwater a waterborne sound implies that they are also able to ear directionally underwater. In fact, Barklow (2004) reported that *H. amphibius* responds to the directionality of underwater sounds. This latter ability implies a specialization of the sound perception pathway. Indeed, for terrestrial mammals, the direction of a sound is determined (1) by the differences of acoustic stimuli received by the two independent ears, and (2) by the interaural time difference (Reysenbach de Haan 1960; Nummela and Thewissen 2008). In water, sound travels five times faster than in air, reducing both interaural time and intensity differences. Intensity difference of the stimuli received by the two ears is reduced because the impedance of the soft tissues of the head is very close to that of water, and the sound travels through the tissues of the head to both ears; they are therefore stimulated at approximately the same time (Reysenbach de Haan 1960). Directional underwater hearing is thus highly limited for most mammals adapted to terrestrial life, which in contrast does not apply to hippos. In aquatic taxa, such as living cetaceans, the ears are acoustically isolated from the rest of the cranium in order to limit the reception of bone-conducted sounds and allow directional sensitivity. In hippos, the drastic reduction of the mastoid part of the petrosal coincides with an almost complete isolation of the petrosal from the other bones of the cranium, as the mastoid process of the petrosal no longer intercalates between the occipital and squamosal bones. O'Leary et al. (O'Leary et al. 2012: Figures 4.1–4.2) illustrated the separation between the petrosal and the squamosal in *Hipppotamus* and *Bothriogenys* and mentioned the importance of this separation for isolating the ear bones from cranial vibrations, a feature already emphasized by Luo and Gingerich (1999). This reduction of the mastoid, accompanied by an isolation of the petrosal from the squamosal, is also observed in *B. onoideus*, therefore suggesting the same adaptation. However, one should mention that a similar reduction of the mastoid is present in *Elomeryx armatus* (O'Leary 2010: Figures 67–71), which is considered terrestrial. Besides, both extant and extinct suoids, also fully terrestrial mammals, present an important reduction of the mastoid as well (Orliac 2012), comparable to what is observed in hippopotamoids. Accordingly, there seems to be no exclusive correlation between mastoid reduction and directional underwater hearing.

Based on Luo and Gingerich's (1999) hypothesis that a "pachyostotic and osteosclerotic" petrosal would have played a substantial role in directional hearing underwater, O'Leary et al. (2012) showed that aquatic and semi-aquatic artiodactyls, including hippos (O'Leary 2010) and extinct cetaceamorphans, had indeed pachyostotic (i.e., hyperinflated) tegmen tympani, by calculating the volume of the tegmen tympani standardized against volume of the petrosal, excluding the mastoid region. Based on a 3D model of the petrosal of MHNT SAF 001, we applied the protocol of O'Leary et al. (2012) to calculate the relative tegmen tympani volume (RTTV) of *Brachyodus onoideus*. The RTTV of the specimen from Saint-Antoine-de-Ficalba equals 0.48, which corresponds to the volume category 3 of O'Leary et al. (2012), i.e. the same as for *Bothriogenys* cf. *gorringei*. This value is slightly inferior to that calculated for *Choeropsis* (RTTV = 0.62; category 4). O'Leary et al. (2012) interpreted the inflation of the tegmen tympani in *Bothriogenys* as a transitional morphology related to underwater hearing. The petrosal of *Brachyodus onoideus* from St-Antoine-de-Ficalba presents a similar hyperinflation of the tegmen tympani and, accordingly, this feature could be another element supporting the specialization of *Brachyodus onoideus* for directional underwater hearing. Still, the precise role of the inflated tegmen tympani in directional underwater hearing remains to determine.

5 Conclusion

The new material from Saint-Antoine-de-Ficalba documents the cranial features of *Brachyodus onoideus*, so far only described in the unpublished thesis of Dineur (1981). The preserved part of the skull is remarkable by the dorsally-protruding orbits, the importance of the postorbital constriction and the small volume of the braincase, the gigantic size of the occipital condyle relative to the other elements of the neurocranium. The cranial morphology of *B. onoideus* from the early Neogene of Europe is similar to that of *B. aequatorialis* from the same period in Africa. In terms of ecology, taken altogether, (1) the disposition of the orifices of the head, (2) the reduced mastoid, isolating the petrosal in the braincase, and (3) the hyperinflated tegmen tympani are arguments supporting a specialization of *Brachyodus onoideus* to an amphibious lifestyle and to underwater directional hearing.

Acknowledgments This material has been collected with the help of the Service Régional d'Aquitaine de l'Institut National de la Recherche Archéologique Préventive (INRAP), the «Archéologies» Association (F. Echasseriaud), the Direction Régionale de l'Equipement d'Aquitaine (E. Brunier), the Entreprise Charier, and the contribution of all the excavation team. Many thanks to L. Costeur for his welcoming access to the collections at the Naturhistorisches Museum, Basel, and to F. Guy for the CT-scan data of *Choeropsis liberiensis* from the collections of the University of Poitiers. We are grateful to O. Erdal for providing us with more than decent photos of the cranium. L. Scherler and one anonymous reviewer considerably improved a previous version of the manuscript. We were particularly moved to participate in this honorary volume, thanks to Damien Becker's (Musée Jurassien des Sciences Naturelles, Porrentruy) invitation. This is ISE-M publication n° 2013-007

References

Aguilar, J.-P., Antoine, P.-O., Crochet, J.-Y., López-Martínez, N., Métais, G., Michaux, J., et al. (2003). Les mammifères du Miocène inférieur de Beaulieu (Bouches-du-Rhône, France), comparaison avec Wintershof-West et le problème de la limite MN3/MN4. *Coloquios de Paleontología, 54*, 1–24.

Antoine, P.-O., Bulot, C., & Ginsburg, L. (2000). Les rhinocérotidés (Mammalia, Perissodactyla) de l'Orléanien (Miocène inférieur) des bassins de la Garonne et de la Loire : intérêt biostratigraphique. *Comptes Rendus de l'Académie des Sciences, sér IIa, 330*, 571–576.

Antoine, P.-O., Duranthon, F., & Tassy, P. (1997). L'apport des grands mammifères (rhinocérotidés, suoïdes, proboscidiens) à la connaissance des gisements du Miocène d'Aquitaine (France) BioChro'M97. *Mémoires et Travaux de l'Institut de Montpellier, École pratique des hautes Études, 21*, 581–590.

Antunes, M., & Ginsburg, L. (2003). The last Anthracothere *Brachyodus onoideus* (Mammalia, Artiodactyla) from westernmost Europe and its extinction. *Ciências da Terra, 15*, 161–172.

Barklow, W. E. (2004). Amphibious communication with sound in hippos, *Hippopotamus* amphibius. *Animal Behavior, 68*, 1125–1132.

Baudelot, S., & Collier, A. (1978). Les faunes miocènes du Haut Armagnac (Gers, France). 1. Les gisements. *Bulletin de la Société d'Histoire Naturelle de Toulouse, 114*, 194–206.

Bentaleb, I., Langlois, C., Martin, C., Iacumin, P., Carré, M., Antoine, P.-O., et al. (2006). Rhinocerotid tooth enamel 18O/16O variability between 23 and 12 Ma in southwestern France. *Comptes Rendus Geoscience, 338*, 172–179.

Boisserie, J.-R., Lihoreau, F., & Brunet, M. (2005). Origins of Hippopotamidae (Mammalia, Cetartiodactyla): towards resolution. *Zoologica Scripta, 34*, 119–143.

Boisserie, J.-R., Lihoreau, F., Orliac, M. J., Fisher, R., Weston, E., & Ducrocq, S. (2010). Morphology and phylogenetic relationships of the earliest known hippopotamids (Cetartiodactyla, Hippopotamidae, Kenyapotaminae). *Zoological Journal of the Linnean Society, 158*, 325–366.

Bulot, C., Antoine, P.-O., & Duranthon, F. (2009). Rongeurs et lagomorphes du Miocène inférieur de Béon 2 (MN4, Montréal-du-Gers, SW France). *Annales de Paléontologie, 95*, 197–215.

Bulot, C., & Ginsburg, L. (1996). Précisions sur l'âge des gisements à mammifères miocènes de Saint-Vincent de Lamonjoie (Lot et Garonne) et de Navère (Gers). *Bulletin du Muséum national d'Histoire Naturelle, 18*, 615–628.

Clementz, M. T., Holroyd, P. A., & Koch, P. L. (2008). Identifying aquatic habitats of herbivorous mammals through stable isotope analysis. *Palaios, 23*, 574–585.

Cuvier, G. (1822). *Recherches sur les ossemens fossiles*. Paris: Edmond d'Ocagne.

de Bruijn, H., Daams, R., Daxner-Höck, G., Fahlbusch, V., Ginsburg, L., Mein, P., et al. (1992). Report of the RCMNS working group on fossil mammals, Reisenburg 1990. *Newsletters on Stratigraphy, 26*, 65–118.

Depéret, C. (1895). Über die Fauna von miozänen Wirbelthieren aus der ersten Mediterranstufe von Eggenburg. *Sitzsungsberichte der Mathematisch-Naturwissen schaftlichen Classe der kaiserlichen Akademie der Wissenschaften in Wien, 104*, 1–22.

Dineur, H. (1981). Le genre *Brachyodus*, Anthracotheriidae (Artiodactyla, Mammalia) du Miocène inférieur d'Europe et d'Afrique. Mémoires des Sciences de la Terre, Université Paris VI. Thèse 3ème Cycle.

Duranthon, F. (1991). Biozonation des molasses continentales oligo-miocènes de la région toulousaine par l'étude des mammifères. Apports à la connaissance du bassin d'Aquitaine. *Comptes Rendus de l'Académie des Sciences, Paris, 313*, 965–970.

Erfurt J., & Métais G. (2007). Endemic European Paleogene artiodactyls. In D. R Prothero, S. E Foss (Eds.), The Evolution of Artiodactyls (pp 59–84). Baltimore: The Johns Hopkins University Press.

Fourtau, R. (1918). *Contributions à l'étude des vertébrés miocènes de l'Egypte*. Egypt: Ministry of Finance Egypt Survey Department.

Gatesy, J., Geisler J. H., Chang J., Buell C., Berta A, Meredith R. W. (2012). A phylogenetic blueprint for a modern whale. *Molecular Phylogenetics and Evolution.* http://dx.doi.org/10.1016/j.ympev.2012.10.012.

Geisler, J. H, Theodor, J. M., Uhen, M. D., Foss, S. E. (2007). Phylogenetic relationships of cetaceans to terrestrial artiodactyls. In D. R Prothero, S. E Foss (Eds.), The Evolution of Artiodactyls (pp 19–31). Baltimore: The Johns Hopkins University Press.

Gentry, A. W., & Hooker, J. J. (1988). The phylogeny of the Artiodactyla. In M. J. Benton (Ed.), *The phylogeny and classification of the Tetrapods* (Vol. 2, pp. 235–272)., Mammals (Systematics Association Special Volume) Oxford: Clarendon.

Gervais, P. (1859). *Zoologie et Paléontologie françaises (animaux vertébrés). Nouvelles recherches sur les animaux vertébrés dont on trouve les ossements enfouis dans le sol de la France et sur leur comparaison avec les espèces propres aux autres régions du globe*. Paris: Arthus Bertrand.

Ginsburg, L. (1990). The faunas and stratigraphical subdivisions of the Orleanian in the Loire Basin (France). In E. H. Lindsay, V. Fahlbusch, & P. Mein (Eds.), *European neogene mammal chronology* (pp. 157–176). New York, NATO ASI Series: Plenum Press.

Ginsburg, L., & Bulot, C. (2000). Le cadre stratigraphique du site de Sansan. *Bulletin du Muséum National d'Histoire naturelle, Paris, 183*, 39–67.

Gray, J. E. (1821). On the natural arrangement of vertebrose animals. *London Medical Repository, 15*, 296–310.

Lihoreau, F. (2003). Systématique et paléoécologie des Anthracotheriidae [Artiodactyla; Suiformes] du Mio-Pliocène de l'Ancien Monde: implications paléobiogéographiques. Ph.D. dissertation, Universite de Poitiers, France.

Lihoreau, F., Ducrocq, S. (2007). Family Anthracotheriidae. In D. R Prothero, S. E Foss (Eds.), The Evolution of Artiodactyls (pp 89–105). Baltimore: The Johns Hopkins University Press.

Lihoreau, F., Ducrocq, S., Antoine, P.-O., Vianey-Liaud, M., Rafaÿ, S., Garcia, G., et al. (2009). First complete skull of *Elomeryx crispus* (Gervais, 1849) and of *Protaceraterium albigense* (Roman, 1912) from a new Oligocene locality near Moissac (SW France). *Journal of Vertebrate Paleontology, 29*, 242–253.

Luo, Z. X., & Gingerich, P. D. (1999). Terrestrial Mesonychia to aquatic Cetacea: transformation of the basicranium and evolution of hearing in whales. *University of Michigan Papers on Paleontology, 31*, 1–98.

McInnes, D. G. (1951). Miocene anthracotheriidae from East Africa. *Fossil Mammals of Africa, 4*, 1–24.

Mein, P. (1989). Updating of MN Zones. In E.H. Lindsay, V. Fahlbusch, & P Mein (Eds.), European Mammal neogene chronology, NATO ASI Series (pp. 73–90).

Montgelard, C., Catzeflis, F., & Douzery, E. (1997). Phylogenetic relationships of artiodactyls and cetaceans as deduced from the comparison of cytochrome b and 12S rRNA mitochondrial sequences. *Molecular Phylogenetics and Evolution, 14*, 550–559.

Nouel, E. (1866). Mémoire sur un nouveau rhinocéros fossile. *Mémoires de la Société Agricole d'Orléans, 8*, 241–250 (1864–1866).

Nummela, S., & Thewissen, J. G. M. (2008). Hearing in aquatic mammals. In S. Nummela & J. G. M. Thewissen (Eds.), *Sensory evolution on the threshold, adaptation in secondarily vertebrates* (pp. 211–226). Berkley and Los Angeles: University of California Press.

O'Leary, M. A. (2010). Anatomical and phylogenetic study of the osteology of the petrosal of extant and extinct artiodactylans (Mammalia) and relatives. *Bulletin of the American Museum of Natural History, 335*, 1–206.

O'Leary, M., Orliac, M. J., Spaulding, M., Gatesy, J. (in press). Artiodactyla. In P. D. Cantino, de Queiroz K., Gauthier J. A. (Eds), Phylonyms: A Companion to the PhyloCode. Berkeley, CA: University of California Press.

O'Leary, M. A., Patel, B. A., & Coleman, M. N. (2012). Endocranial petrosal anatomy of *Bothriogenys* (Mammalia, Artiodactyla, Anthracotheriidae) and petrosal volume and density comparisons among aquatic and terrestrial artiodactyls and outgroups. *Journal of Paleontology, 86*, 44–50.

Orliac, M. J. (2012). Osteology of the petrosal bone of Suoidea (Artiodactyla, Mammalia). *Journal of Systematic Palaeontology,*. doi:10.1080/14772019.2012.704409.

Orliac, M. J., Boisserie, J.-R., MacLatchy, L., & Lihoreau, F. (2010). Earliest Miocene hippopotamids constrain phylogenetic and spaciotemporal settings of hippopotamid origin. *Proceedings of the National Academy of Science, USA, 107*, 11871–11876.

Owen, R. (1848). *On the Archetype and Homologies of the Vertebrate Skeleton*. Taylor, London: R. Taylor and J.

Pickford, M. (1991). Revision of the Neogene Anthracotheriidae of Africa. In M. J. Salem (Ed.), *The Geology of Libya* (pp. 1491–1525). Amsterdam: Elsevier.

Reinach, A. von (1900). Schildkrötenreste im Mainzer Tertiärbecken und in benachbarten, ungefähr gleichalterigen Ablagerungen. *Abhandlungen aus den Senckenberg Naturkunde Gesellschaft, 28*, 1–153.

Reysenbach de Haan, F. W. (1960). Some aspects of mammalian hearing under water. *Proceedings of the Royal Society of London, B, 152*, 54–62.

Roman, F., & Viret, J. (1930). Le Miocène continental de l′Armagnac et le gisement Burdigalien de La Romieu (Gers). Mémoires de la Société Géologique de France, Nouvelle série, *21*, 1–67.

Scherler, L. (2011). Terrestrial paleoecosystems of large mammals (Tapiridae, Anthracotheriidae, Suoidea) from the Early Oligocene to the Early Miocene in the Swiss Molasse Basin: biostratigraphy, biogeochemistry, paleobiogeography and paleoecology. Unpublished PhD Thesis, University of Fribourg.

Scott, W. B. (1940). The mammalian fauna of the White River Oligocene, Part IV: Artiodactyla. *Philadelphia American Philosophical Society Transactions, New Series, 28*, 363–746.

Spaulding, M., O'Leary, M. A., & Gatesy, J. (2009). Relationships of Cetacea (Artiodactyla) among mammals: increased taxon sampling alters interpretations of key fossils and character evolution. *PLoS ONE, 4*, e7062.

Studer, T. von (1895). Die Säugetierreste aus den marinen Molasseablagerungen von Brüttelen. *Schweizerische paläontologische Abhandlungen, 22*, 1–47.